

Electrochemical and Homogeneous Exchange Kinetics for Transition-Metal Aquo Couples: Anomalous Behavior of Hexaaquoiron(III/II)

JOSEPH T. HUPP and MICHAEL J. WEAVER*

Received July 16, 1982

Rate data for electrochemical and homogeneous redox reactions involving $\text{Ru}_{\text{aq}}^{3+/2+}$, $\text{V}_{\text{aq}}^{3+/2+}$, $\text{Fe}_{\text{aq}}^{3+/2+}$, $\text{Eu}_{\text{aq}}^{3+/2+}$, and $\text{Cr}_{\text{aq}}^{3+/2+}$ redox couples (where "aq" represents aquo ligands) have been analyzed and compared by using the rate relations due to Marcus in order to ascertain how the kinetics of outer-sphere electron exchange are dependent upon the metal redox center. The work-corrected rate constants for electrochemical exchange at mercury electrodes, k_{ex}^e , were found to be in uniformly good agreement with the rate constants for homogeneous self-exchange, k_{ex}^h , extracted from cross-reaction data involving outer-sphere coreactants, yielding the reactivity sequence $\text{Ru}_{\text{aq}}^{3+/2+} > \text{V}_{\text{aq}}^{3+/2+} > \text{Fe}_{\text{aq}}^{3+/2+} \approx \text{Eu}_{\text{aq}}^{3+/2+} > \text{Cr}_{\text{aq}}^{3+/2+}$. However, the measured rate constant for $\text{Fe}_{\text{aq}}^{3+/2+}$ self-exchange is not consistent with this sequence, being at least 10^3 -fold larger than the values of k_{ex}^h extracted from both the homogeneous cross-reaction and electrochemical data. The latter values of k_{ex}^h and also k_{ex}^e are in harmony with the relative inner-shell barriers for $\text{Fe}_{\text{aq}}^{3+/2+}$ and $\text{Ru}_{\text{aq}}^{3+/2+}$ calculated from crystallographic structural data. The above reactivity sequence is also consistent with the relative structural changes accompanying electron transfer as monitored by the corresponding reaction entropies.

Recent developments in the theory of outer-sphere electron transfer have focused attention on the contribution of inner-shell reorganization, ΔG_{is}^* , to the intrinsic free energy barrier for electron exchange ΔG_{ex}^* .¹⁻⁶ Transition-metal redox couples containing only aquo ligands, of the type $\text{M}_{\text{aq}}^{3+} + e^- \rightleftharpoons \text{M}_{\text{aq}}^{2+}$ where $\text{M} = \text{Ru}, \text{Fe}, \text{Co}, \text{V},$ and Eu , form an especially interesting series in which to compare the theoretical predictions with experiment since they exhibit large differences in redox reactivity that are likely to be due primarily to the influences of the metal electronic structure upon ΔG_{is}^* . Some of these reactions exhibit remarkably small exchange rates.⁷

Experimental estimates of ΔG_{ex}^* can be obtained from the rates of homogeneous self-exchange or electrochemical exchange or, less directly, from the kinetics of suitable homogeneous cross-reactions with other redox couples having self-exchange kinetics that are known or can be estimated.^{8,9} Relationships between the kinetics of these reactions are given by the well-known equations derived from an adiabatic electron-transfer model:^{8,9}

$$k_{\text{ex}}^e/A_e \leq (k_{\text{ex}}^h/A_h)^{1/2} \quad (1)$$

and

$$k_{12}^h = (k_{11}^h k_{22}^h K_{12} f)^{1/2} \quad (2a)$$

where

$$\log f = (\log K_{12})^2 / [4 \log (k_{11}^h k_{22}^h / A_h^2)] \quad (2b)$$

In eq 1, k_{ex}^e and k_{ex}^h are the corresponding rate constants for electrochemical exchange and homogeneous self-exchange for a given redox couple and A_e and A_h are the electrochemical and homogeneous frequency factors, respectively. In eq 2, k_{11}^h and k_{22}^h are the rate constants for the parent self-exchange reactions corresponding to a homogeneous cross-reaction having a rate constant k_{12}^h and equilibrium constant K_{12} . All

these rate constants are presumed to be corrected for work terms. A given rate constant for homogeneous self-exchange k_{ex}^h can be related to the corresponding intrinsic barrier ΔG_{ex}^* by^{1,9}

$$k_{\text{ex}}^h = \kappa A_h \exp(-\Delta G_{\text{ex}}^* / RT) \quad (3)$$

where κ is an electronic transmission coefficient. The rate constant for electrochemical exchange k_{ex}^e can also be related to ΔG_{ex}^* by

$$k_{\text{ex}}^e = \kappa A_e \exp(-\Delta G_{\text{ex},e}^* / RT) \quad (4a)$$

$$k_{\text{ex}}^e = \kappa A_e \exp[-(\Delta G_{\text{ex}}^* + C) / 2RT] \quad (4b)$$

where $\Delta G_{\text{ex},e}^*$ is the intrinsic electrochemical barrier. The factor 2 arises in eq 4b because only one reactant is required to be activated in the electrochemical reaction, rather than a pair of reactants as in the homogeneous case. The contributions to ΔG_{ex}^* and $\Delta G_{\text{ex},e}^*$ arising from inner-shell (i.e., metal-ligand) reorganization, ΔG_{is}^* and $\Delta G_{\text{is},e}^*$, respectively, are therefore related by $\Delta G_{\text{is}}^* = 2\Delta G_{\text{is},e}^*$. The relationship between the components of ΔG_{ex}^* and $\Delta G_{\text{ex},e}^*$ due to outer-shell (i.e., solvent) reorganization, ΔG_{os}^* and $\Delta G_{\text{os},e}^*$, is somewhat less straightforward. According to a dielectric continuum treatment, these quantities are given by^{8,9}

$$\Delta G_{\text{os}}^* = \frac{e^2}{4} \left(\frac{1}{a} - \frac{1}{R_h} \right) \left(\frac{1}{\epsilon_{\text{op}}} - \frac{1}{\epsilon_s} \right) \quad (5a)$$

$$\Delta G_{\text{os},e}^* = \frac{e^2}{8} \left(\frac{1}{a} - \frac{1}{R_c} \right) \left(\frac{1}{\epsilon_{\text{op}}} - \frac{1}{\epsilon_s} \right) \quad (5b)$$

where e is the electronic charge, a is the (average) reactant radius, ϵ_{op} and ϵ_s are the optical and static dielectric constants, R_h is the close contact distance between the homogeneous redox centers, and R_c is twice the distance between the reactant and the electrode surface.⁹ It is generally expected for outer-sphere reactions that $R_c > R_h$; therefore, $\Delta G_{\text{os}}^* < 2\Delta G_{\text{os},e}^*$. The quantity C in eq 4b accounts for this inequality, which is also the origin of the inequality sign in eq 1; from eq 4 and 5

$$C = \frac{e^2}{4} \left(\frac{1}{R_h} - \frac{1}{R_c} \right) \left(\frac{1}{\epsilon_{\text{op}}} - \frac{1}{\epsilon_s} \right) \quad (6)$$

Equation 1 can therefore be written in the more general form

$$2 \log (k_{\text{ex}}^e / A_e) = \log (k_{\text{ex}}^h / A_h) - C / 2.303RT \quad (7)$$

- (1) B. S. Brunschwig, J. Logan, M. D. Newton, and N. Sutin, *J. Am. Chem. Soc.*, **102**, 5798 (1980).
- (2) M. D. Newton, *Int. J. Quantum Chem., Quantum Chem. Symp.*, No. **14**, 363 (1980).
- (3) E. Buhks, M. Bixon, J. Jortner, and G. Navon, *Inorg. Chem.*, **18**, 2014 (1979).
- (4) P. Siders and R. A. Marcus, *J. Am. Chem. Soc.*, **103**, 741 (1981).
- (5) J. Ulstrup, "Charge Transfer Processes in Condensed Media", Springer-Verlag, West Berlin, 1979.
- (6) P. P. Schmidt, *Spec. Period. Rep.: Electrochem.*, **5**, Chapter 2 (1975); **6**, Chapter 4 (1977).
- (7) See, for example, R. G. Linck in "Homogeneous Catalysis", G. N. Schrauzer, Ed., Marcel Dekker, New York, 1971, Chapter 7.
- (8) R. A. Marcus, *J. Phys. Chem.*, **67**, 853 (1963).
- (9) R. A. Marcus, *J. Chem. Phys.*, **43**, 679 (1965).

For a series of reactants having similar sizes and structures, as for the present aquo couples, R_h and R_c and hence C should remain approximately constant.

It is desirable to obtain a self-consistent set of experimental values of k_{ex}^h or k_{ex}^c for comparison with theoretical predictions obtained from calculated values of ΔG_{ex}^* by using eq 3 and 4. This task is less straightforward than is commonly presumed for two reasons. First, the experimental values of k_{ex}^h or k_{ex}^c may not refer to outer-sphere pathways since (except for $Ru_{aq}^{3+/2+}$) at least one of the aquo reaction partners is substitutionally labile so that more facile inner-sphere pathways may provide the dominant mechanism. Second, values of k_{ex}^h derived by using eq 2 from rate constants for appropriate outer-sphere cross-reactions not only rely on the availability of values of k_{ex}^h for the coreacting redox couple along with values of K_{12} but also depend on the applicability of this relation.^{10,11} The resulting estimates of k_{ex}^h for different redox couples are often difficult to compare since large systematic errors can be introduced by the use of cross-reaction data involving structurally different coreactants, inappropriate electrode potential data, etc.

In spite of their direct relationship to the desired intrinsic barriers, electrochemical exchange rate data have seldom been utilized for this purpose. One reason is that these data have commonly been gathered at ill-defined solid surfaces where the work terms arising from double-layer effects are large and unknown, precluding quantitative intercomparison of the results. However, we have determined accurate electrochemical rate data for $V_{aq}^{3+/2+}$, $Cr_{aq}^{3+/2+}$, $Eu_{aq}^{3+/2+}$, $Ru_{aq}^{3+/2+}$, and $Fe_{aq}^{3+/2+}$ at the mercury-aqueous interface under conditions where the work terms are small and can be estimated with confidence.¹²⁻¹⁴ The interactions between the reactant and the metal surface are likely to be weak and nonspecific, so that the electrode can be viewed as providing an inert electron source or sink that does not influence the electron-transfer barrier. This allows information on the electron-transfer barrier to be gathered for *individual* redox couples as a function of the thermodynamic driving force. Such information is largely inaccessible from the kinetics of homogeneous electron transfer.¹⁵

In the present paper, suitable rate data for electrochemical and homogeneous reactions involving aquo redox couples are analyzed and compared with use of eq 2 and 7 in order to ascertain as unambiguously as possible how the kinetics of outer-sphere electron exchange depend on the metal redox center.

Rate Constants for Electrochemical Exchange

Table I contains a summary of rate parameters for the electrochemical exchange of $Ru_{aq}^{3+/2+}$, $V_{aq}^{3+/2+}$, $Fe_{aq}^{3+/2+}$, $Eu_{aq}^{3+/2+}$, and $Cr_{aq}^{3+/2+}$ at the mercury-aqueous interface, using potassium hexafluorophosphate and lanthanum perchlorate supporting electrolytes. These experimental conditions minimized the extent of the electrostatic double-layer effect upon the apparent rate constants for electrochemical exchange, $k_{ex}^c(\text{app})$ (i.e., the "standard" rate constants measured at the formal potential E_f for the redox couple concerned), enabling values of the work-corrected rate constants, k_{ex}^c , to be evaluated with confidence by using¹⁶

$$\ln k_{ex}^c = \ln k_{ex}^c(\text{app}) + \frac{F}{RT}(Z_r - \alpha_{cor})\phi_d \quad (8)$$

Table I. Kinetics and Related Thermodynamic Parameters for the Electrochemical Exchange of Some M(III/II) Aquo Redox Couples at the Mercury-Aqueous Interface at 25 °C

redox couple	electrolyte ^a	E_f^b		$k_{ex}^c(\text{app})^c$ cm s ⁻¹	ϕ_d^d mV	k_{ex}^e cm s ⁻¹
		mV vs. SCE	mV			
$Ru_{aq}^{3+/2+}$	0.4 M KPF ₆	-20	5 × 10 ⁻³	10	~2 × 10 ⁻²	
$V_{aq}^{3+/2+}$	0.4 M KPF ₆	-472	1.5 × 10 ⁻³	-5	1 × 10 ⁻³	
$Fe_{aq}^{3+/2+}$	0.4 M KPF ₆	495	2 × 10 ^{-5 f}		~1 × 10 ⁻⁴	
$Eu_{aq}^{3+/2+}$	0.4 M KPF ₆	-625	6 × 10 ⁻⁴	-20	8 × 10 ⁻⁵	
	0.04 M La(ClO ₄) ₃	-625	3.5 × 10 ⁻⁴			
$Cr_{aq}^{3+/2+}$	0.4 M KPF ₆	-655	2 × 10 ⁻⁵	-25	2 × 10 ⁻⁶	
	0.04 M La(ClO ₄) ₃	-655	1.0 × 10 ⁻⁵			

^a Electrolyte contained sufficient (>5-10 mM) acid to suppress significant deprotonation of $M(OH)_2^{3+}$. ^b Formal potential for redox couple in stated electrolyte at 25 °C. Values taken from ref 20 and supplemented by unpublished data from this laboratory. ^c Measured (apparent) value of rate constant at mercury electrode in stated electrolyte at formal potential; obtained from ref 12-14. ^d Approximate potential across diffuse layer at E_f^b in given electrolyte; obtained or estimated from ref 12-14. ^e Work-corrected rate constant for electrochemical exchange; obtained from $k_{ex}^c(\text{app})$ and ϕ_d by using eq 8. ^f Estimated as indicated in the text.

where Z_r is the reactant charge number, α_{cor} is the work-corrected cathodic transfer coefficient, and ϕ_d is the potential drop across the diffuse layer. Details of this procedure are given in ref 12-14. The KPF₆ electrolyte provides an especially suitable medium for this purpose. This is because ϕ_d is small over a wide potential range positive of the potential of zero charge (-440 mV vs. SCE) since the positive electronic charge density at the electrode is matched approximately by the charge density due to specifically adsorbed PF₆⁻ anions.^{13,16} The rate data in Table I all refer to acid-independent pathways. In contrast to homogeneous reactions between aquo cations, the rates of most of these reactions are independent of pH at values (≤pH 2.5) below which the formation of hydroxo complexes is unimportant. The single exception is $V_{aq}^{3+/2+}$, which exhibits a significant inverse acid-dependent pathway at pH ≥ 1.¹⁷

The formal potential for $Fe_{aq}^{3+/2+}$ is too positive (495 mV vs. SCE in 0.4 M KPF₆) to allow rate measurements in the vicinity of E_f to be made at mercury since anodic dissolution of the electrode occurs beyond about 375 mV. However, the electroreduction of Fe_{aq}^{3+} was found to be sufficiently irreversible so that cathodic dc and normal-pulse polarograms were obtained over the potential range 300-0 mV, yielding values of k_{app} in 0.4 M KPF₆ of 4 × 10⁻⁴ cm s⁻¹ at 300 mV and 0.1 cm s⁻¹ at 0 mV vs. SCE. Extrapolation of the cathodic Tafel plots (i.e., $\ln k_{app}^c$ vs. E , where k_{app}^c is the apparent cathodic rate constant) was therefore required in order to extract $k_{ex}^c(\text{app})$. However, this procedure can be applied with confidence: the work-corrected cathodic transfer coefficients, α_{cor} , for several other aquo couples are close to 0.50 (±0.02) over a wide range of cathodic overpotentials.¹³ The value of the observed transfer coefficient α_{app} (0.48) for Fe_{aq}^{3+} reduction in 0.4 M KPF₆ indicates that the potential dependence of the double-layer effects is likely to be small, as expected.¹³ Consequently, the resulting value of $k_{ex}^c(\text{app})$, ~2 × 10⁻⁵ cm s⁻¹, is likely to be within a factor of 2- to 5-fold of k_{ex}^c ; we have therefore set an upper limit of 1 × 10⁻⁴ cm s⁻¹ for k_{ex}^c in Table I.

These values of $k_{ex}^c(\text{app})$ and k_{ex}^c are smaller than those commonly reported for $Fe_{aq}^{3+/2+}$ at platinum and gold elec-

- (10) M. Chou, C. Creutz and N. Sutin, *J. Am. Chem. Soc.*, **99**, 5615 (1977).
 (11) M. J. Weaver and E. L. Yee, *Inorg. Chem.*, **19**, 1936 (1980).
 (12) M. J. Weaver, *J. Phys. Chem.*, **84**, 568 (1980).
 (13) P. D. Tyma and M. J. Weaver, *J. Electroanal. Chem. Interfacial Electrochem.*, **111**, 195 (1980).
 (14) M. J. Weaver, P. D. Tyma, and S. M. Nettles, *J. Electroanal. Chem. Interfacial Electrochem.*, **114**, 53 (1980).
 (15) M. J. Weaver and J. T. Hupp, *ACS Symp. Ser.*, No. **198**, 181 (1982).

- (16) M. J. Weaver, *J. Electroanal. Chem. Interfacial Electrochem.*, **93**, 231 (1978).
 (17) J. Lipkowski, A. Czerwinski, E. Cieszyńska, Z. Galus, and J. Sobkowski, *J. Electroanal. Chem. Interfacial Electrochem.*, **119**, 261 (1981).

Table II. Estimation of Work-Corrected Rate Constants k_{ex}^{h} ($\text{M}^{-1} \text{s}^{-1}$) at 25 °C for $\text{Fe}_{\text{aq}}^{3+/2+}$, $\text{Ru}_{\text{aq}}^{3+/2+}$, $\text{V}_{\text{aq}}^{3+/2+}$, $\text{Eu}_{\text{aq}}^{3+/2+}$, and $\text{Cr}_{\text{aq}}^{3+/2+}$ Self-Exchange from Selected Cross-Reaction Data

cross-reaction ^r	K_{12}^a	$k_{12}^{\text{h}}(\text{app})^f$	$k_{12}^{\text{h}m}$	$k_{12}^{\text{h}n}$	f^p	$k_{\text{ex}}^{\text{h}q}$
$\text{Fe}_{\text{aq}}^{3+} + \text{Fe}_{\text{aq}}^{2+}$	1.0	4 (0.55)	15		1.0	15
$\text{Fe}_{\text{aq}}^{3+} + \text{Ru}_{\text{aq}}^{2+}$	5×10^8	2.3×10^3 (1)	7×10^3	$\sim 50^o$	0.18	$\sim 1 \times 10^{-3}$
$\text{Fe}_{\text{aq}}^{3+} + \text{Ru}(\text{NH}_3)_5\text{py}^{2+}$	$1.5 \times 10^7^b$	5.8×10^4 (1)	1.7×10^5	1.5×10^6	0.23	6×10^{-3}
$\text{Fe}_{\text{aq}}^{3+} + \text{Ru}(\text{NH}_3)_4\text{bpy}^{2+}$	$4.5 \times 10^3^b$	7.2×10^3 (1) ^g	2×10^4	$\sim 1 \times 10^7^k$	0.73	1.2×10^{-2}
$\text{Fe}_{\text{aq}}^{3+} + \text{Co}(\text{phen})_3^{2+}$	1.2×10^6	5.3×10^2 (1) ^h	1.6×10^3	150	0.40	3.5×10^{-2}
$\text{Os}(\text{bpy})_3^{3+} + \text{Fe}_{\text{aq}}^{2+}$	80 ^c	1.4×10^3 (0.5) ⁱ	3×10^3	$(\sim 1 \times 10^9)$	0.89	$\sim 2 \times 10^{-4}$
$\text{Fe}(\text{bpy})_3^{3+} + \text{Fe}_{\text{aq}}^{2+}$	5.5×10^5	2.7×10^4 (0.5) ^j	6×10^4	$(\sim 1 \times 10^9)$	0.38	$\sim 3 \times 10^{-5}$
$\text{Fe}(\text{phen})_3^{3+} + \text{Fe}_{\text{aq}}^{2+}$	1.2×10^6	3.7×10^4 (0.5) ^j	1.5×10^5	$(\sim 1 \times 10^9)$	0.33	$\sim 5 \times 10^{-5}$
$\text{Ru}(\text{bpy})_3^{3+} + \text{Fe}_{\text{aq}}^{2+}$	1.8×10^9	7.2×10^5 (1)	2×10^6	$\sim 1 \times 10^9$	0.068	$\sim 3 \times 10^{-4}$
$\text{Ru}_{\text{aq}}^{3+} + \text{V}_{\text{aq}}^{2+}$	5.8×10^7	2.8×10^2 (1) ^d	9×10^2	3×10^{-2}	0.25	2
$\text{Ru}_{\text{aq}}^{3+} + \text{Ru}(\text{NH}_3)_6^{2+}$	6×10^2	1.4×10^4 (1) ^d	4×10^4	$\sim 5 \times 10^4$	0.78	70
$\text{Co}(\text{phen})_3^{3+} + \text{Ru}_{\text{aq}}^{2+}$	4.2×10^2	53 (1) ^d	1.5×10^2	160	0.78	0.4
$\text{Ru}(\text{NH}_3)_5\text{py}^{3+} + \text{Ru}_{\text{aq}}^{2+}$	35 ^b	1.1×10^4 (1) ^d	3.5×10^4	1.5×10^6	0.92	25
$\text{Ru}(\text{NH}_3)_5\text{isn}^{3+} + \text{Ru}_{\text{aq}}^{2+}$	6.5×10^{2d}	5.5×10^4 (1) ^d	1.5×10^5	1.5×10^6 ^g	0.76	30
$\text{V}_{\text{aq}}^{3+} + \text{V}_{\text{aq}}^{2+}$	1.0	1.5×10^2 (2)	3×10^{-2}		1.0	3×10^{-2}
$\text{V}_{\text{aq}}^{3+} + \text{Cr}(\text{bpy})_3^{2+}$	1.2 ^e	4.2×10^2 (1) ^k	1×10^3	$(\sim 1 \times 10^9)$	1.0	1×10^{-3}
$\text{Co}(\text{en})_3^{3+} + \text{V}_{\text{aq}}^{2+}$	2.5	7×10^{-4} (1)	2.5×10^{-3}	2.5×10^{-4}	1.0	6×10^{-2}
$\text{Ru}(\text{NH}_3)_6^{3+} + \text{V}_{\text{aq}}^{2+}$	1×10^5	1.5×10^3 (0.5)	2×10^4	$\sim 5 \times 10^4$	0.49	0.15
$\text{Co}(\text{bpy})_3^{3+} + \text{V}_{\text{aq}}^{2+}$	1.3×10^9	1.1×10^3 (2)	2×10^3	80	0.15	3×10^{-4}
$\text{Co}(\text{phen})_3^{3+} + \text{V}_{\text{aq}}^{2+}$	2.5×10^{10}	4×10^3 (1)	1.5×10^4	150	0.08	1×10^{-3}
$\text{Ru}(\text{NH}_3)_5\text{py}^{3+} + \text{V}_{\text{aq}}^{2+}$	$2 \times 10^9^b$	3×10^5 (1)	1×10^6	1.5×10^6	0.08	4×10^{-3}
$\text{V}_{\text{aq}}^{3+} + \text{Eu}_{\text{aq}}^{2+}$	3.5×10^2	9×10^{-3} (2)	2×10^{-2}	3×10^{-2}	0.88	4.5×10^{-5}
$\text{Co}(\text{en})_3^{3+} + \text{Eu}_{\text{aq}}^{2+}$	7.5×10^2	$\sim 5 \times 10^{-3}$ (1)	$\sim 1 \times 10^{-2}$	2.5×10^{-4}	0.86	$\sim 5 \times 10^{-4}$
$\text{Ru}(\text{NH}_3)_6^{3+} + \text{Eu}_{\text{aq}}^{2+}$	3.5×10^7	2.3×10^3 (1)	7×10^3	$\sim 5 \times 10^4$	0.25	1×10^{-4}
$\text{Co}(\text{phen})_3^{3+} + \text{Eu}_{\text{aq}}^{2+}$	1.3×10^{13}	9×10^2 (1) ^k	2.5×10^3	150	0.03	1×10^{-7}
$\text{Ru}(\text{NH}_3)_5\text{py}^{3+} + \text{Eu}_{\text{aq}}^{2+}$	$7 \times 10^{11}^b$	5.4×10^4 (1)	1.5×10^5	1.5×10^6	0.03	7×10^{-7}
$\text{Eu}_{\text{aq}}^{3+} + \text{Cr}_{\text{aq}}^{3+}$	3.5	$\sim 2 \times 10^{-5}$ (0.5)	8×10^{-5}	2×10^{-4}	1.0	9×10^{-6}
$\text{Co}(\text{en})_3^{3+} + \text{Cr}_{\text{aq}}^{2+}$	2.5×10^3	3×10^{-4} (1)	1×10^{-3}	2.5×10^{-4}	0.82	2×10^{-6}
$\text{Ru}(\text{NH}_3)_6^{3+} + \text{Cr}_{\text{aq}}^{2+}$	1.2×10^8	2×10^{-4}	2×10^3	$\sim 5 \times 10^4$	0.22	3×10^{-6}
$\text{Co}(\text{phen})_3^{3+} + \text{Cr}_{\text{aq}}^{2+}$	6×10^{13}	30 (1) ^h	90	150	0.03	3×10^{-11}
$\text{Ru}(\text{NH}_3)_5\text{py}^{3+} + \text{Cr}_{\text{aq}}^{2+}$	$2.5 \times 10^{12}^b$	3.4×10^3 (1)	1×10^4	1.5×10^6	0.10	3×10^{-10}

^a Formal equilibrium constant for cross-reaction; calculated from $\ln K_{12} = (F/RT)(E_{\text{red}}^{\text{f}} - E_{\text{ox}}^{\text{f}})$, where $E_{\text{red}}^{\text{f}}$ and E_{ox}^{f} are the formal potentials of the redox couples undergoing reduction and oxidation, respectively, in the range of ionic strengths ($\mu \approx 0.2$ –1) employed for the kinetics measurements. Values of E^{f} for aquo couples are given in Table I; values for other couples are taken from ref 20 unless otherwise noted. ^b From ref 21. ^c E^{f} for $\text{Os}(\text{bpy})_3^{3+/2+}$ is 619 mV vs. SCE; $\mu = 0.1$ [F. P. Dwyer, N. A. Gibson, and E. C. Gyarfás, *J. Proc. R. Soc. N.S.W.* **84**, 80 (1950)]. ^d From ref 25. ^e E^{f} for $\text{Cr}(\text{bpy})_3^{3+/2+}$ is -480 mV vs. SCE; $\mu = 0.1$ [S. Sahami and M. J. Weaver, *J. Electroanal. Chem. Interfacial Electrochem.*, **122**, 155 (1981)]. ^f Measured rate constant for listed cross-reaction at 25 °C and ionic strength given in parentheses; values taken from sources quoted in ref 11 unless otherwise noted. ^g G. M. Brown, H. S. Krentzien, M. Abe, and H. Taube, *Inorg. Chem.*, **18**, 3374 (1979). ^h T. J. Przystas and N. Sutin, *J. Am. Chem. Soc.*, **95**, 5545 (1973). ⁱ B. M. Gordon, L. L. Williams, and N. Sutin, *ibid.*, **83**, 2061 (1961). ^j M. H. Ford-Smith and N. Sutin, *ibid.*, **83**, 1830 (1961). ^k Reference 10. ^l R. G. Gaunder and H. Taube, *Inorg. Chem.*, **9**, 2627 (1970). ^m Rate constant for cross-reaction, after correction for work terms as outlined in ref 11. ⁿ Work-corrected value of k_{ex}^{h} for coreactant; taken from ref 11 unless otherwise noted. Values for low-spin $\text{M}(\text{bpy})_3^{3+/2+}$ couples ($1 \times 10^9 \text{ M}^{-1} \text{ s}^{-1}$) are estimated (see text). ^o From this work. ^p Quadratic driving force factor; defined by eq 2b. ^q Work-corrected rate constant for self-exchange of aquo redox couple; obtained from corresponding values of K_{12} , k_{12}^{h} , and k_{22}^{h} by using eq 2. ^r py = pyridine, en = ethylenediamine, and isn = isonicotinamide.

trodes.^{18a} However, cathodic voltammograms that are highly irreversible (half-wave potential $E_{1/2} \approx 0$ mV vs. SCE), yielding similarly small values of $k_{\text{ex}}^{\text{h}}(\text{app})$ ($\sim 10^{-5} \text{ cm}^2 \text{ s}^{-1}$), have recently been obtained at platinum and gold in perchlorate media from which halide impurities had been rigorously excluded.^{18b} The larger values of $k_{\text{ex}}^{\text{h}}(\text{app})$ are therefore due to the presence of halide-catalyzed, possibly inner-sphere, pathways.¹⁹ Rate measurements at dropping-mercury electrodes are not susceptible to such difficulties since the surface is continuously renewed and adsorbs most anions much more weakly than do noble metals.

The electrochemical reactivities of $\text{Fe}_{\text{aq}}^{3+/2+}$ and $\text{Ru}_{\text{aq}}^{3+/2+}$ provide an interesting comparison. At the formal potential for $\text{Ru}_{\text{aq}}^{3+/2+}$ in 0.4 M KPF₆, -20 mV vs. SCE, the observed rate constant for electroreduction of $\text{Fe}_{\text{aq}}^{3+}$ is $0.15 (\pm 0.05) \text{ cm}^2 \text{ s}^{-1}$. This value is only moderately (30-fold) larger than that for $\text{Ru}_{\text{aq}}^{3+}$ reduction at the same potential, $5 (\pm 2) \times 10^{-3} \text{ cm}^2 \text{ s}^{-1}$, despite the enormous cathodic overpotential (515 mV, corresponding to an equilibrium constant of 5×10^8) for the former reaction. Since these rate constants were obtained under the same conditions and the reactants are of very similar structure, the work terms will be essentially identical. Any reasonable driving force correction for $\text{Fe}_{\text{aq}}^{3+}$ reduction therefore must yield a value of k_{ex}^{h} ca. 10^3 -fold smaller than for $\text{Ru}_{\text{aq}}^{3+}$ reduction, irrespective of the work term corrections upon the individual rate constants. From eq 7, this results in a corresponding estimate of k_{ex}^{h} that is ca. 10^5 -fold smaller for the former reaction (vide infra).

Rate Constants for Electron Exchange from Homogeneous Cross-Reaction Kinetics

Rate Constants for Electron Exchange from Homogeneous Cross-Reaction Kinetics

Table II summarizes pertinent rate and equilibrium data for the acid-independent pathways for cross-reactions involving $\text{Fe}_{\text{aq}}^{3+/2+}$, $\text{Ru}_{\text{aq}}^{3+/2+}$, $\text{V}_{\text{aq}}^{3+/2+}$, $\text{Eu}_{\text{aq}}^{3+/2+}$, and $\text{Cr}_{\text{aq}}^{3+/2+}$, together with the values of k_{ex}^{h} for these couples resulting from the application of eq 2. The rate constants for the cross-reactions, k_{12}^{h} , and for self-exchange of the various coreactants, k_{22}^{h} , listed in Table II are taken from literature data; they are corrected for Debye-Hückel work terms as described in ref 11 (see the footnotes to Table II and ref 11 for the data sources). The measured values of k_{12}^{h} , $k_{12}^{\text{h}}(\text{app})$, are also

(18) (a) For example, see D. H. Angell and T. Dickinson, *J. Electroanal. Chem. Interfacial Electrochem.*, **35**, 55 (1972). (b) D. C. Johnson and E. W. Resnick, *Anal. Chem.*, **49**, 1918; J. Weber, Z. Samec, and V. Marecek, *J. Electroanal. Chem. Interfacial Electrochem.*, **87**, 271 (1978).

(19) S. W. Barr, K. L. Guyer, and M. J. Weaver, *J. Electroanal. Chem. Interfacial Electrochem.*, **111**, 41 (1980).

listed, with the ionic strength at which they were determined in parentheses. The equilibrium constants K_{12} given in Table II were obtained from measurements of formal potentials for the appropriate redox couples at ionic strengths comparable ($0.1 \leq \mu \leq 1$) to those at which the kinetic data were gathered. (Most of these formal potentials were obtained in our laboratory by using cyclic voltammetry.^{20,21} The uniform use of these data avoids the substantial errors that can arise if literature electrode potential values gathered under disparate conditions are employed to calculate K_{12} , as is commonly done.) Although values of k_{ex}^h for some of the polypyridine redox couples utilized in Table II [$\text{Fe}(\text{bpy})_3^{3+/2+}$, $\text{Fe}(\text{phen})_3^{3+/2+}$, $\text{Os}(\text{bpy})_3^{3+/2+}$, and $\text{Cr}(\text{bpy})_3^{3+/2+}$ ($\text{bpy} = 2,2'$ -bipyridine, $\text{phen} = 1,10$ -phenanthroline)] have not been determined, they are assumed to be comparable to that obtained for $\text{Ru}(\text{bpy})_3^{3+/2+}$, ca. $1 \times 10^9 \text{ M}^{-1} \text{ s}^{-1}$.^{10,22} The inner-shell reorganization energies for all these couples are likely to be close to zero since they uniformly involve the transfer of a delocalized t_{2g} electron.¹⁰

Detailed inspection of Table II reveals that work-corrected values of k_{ex}^h are obtained for each aquo redox couple that are reasonably constant (mostly within ca. 10-fold of each other), at least for cross-reactions having relatively small driving forces (e.g., $K_{12} < 1 \times 10^6$, $f \geq 0.2$).¹¹ There are good reasons to prefer such weakly exoergic cross-reactions for extracting values of k_{ex}^h by using eq 2. The assumptions made in deriving eq 2, that the reactions are adiabatic ($\kappa \approx 1$), the work terms are nonspecific, and the reactant and product free energy profiles are harmonic, are questionable, especially for reactions involving aquo cations.^{11,13,15} However, these factors have only a minor influence upon its applicability to reactions having small driving forces providing that the work terms and κ are comparable for the corresponding self-exchange reactions and cross-reactions.^{10,11} Indeed, progressively smaller estimates of k_{ex}^h are generally determined by using eq 2 from cross-reactions having increasingly large driving forces. These discrepancies have been attributed to the influence of unfavorable specific work terms,¹¹ anharmonicity,¹⁵ and nonadiabaticity.¹⁰

The extraction of relative values of k_{ex}^h for $\text{V}_{aq}^{3+/2+}$, $\text{Eu}_{aq}^{3+/2+}$, and $\text{Cr}_{aq}^{3+/2+}$ is facilitated by the proximity of the formal potentials for these couples (-472 , -625 , and -655 mV vs. SCE; $\mu \approx 0.5$; Table I). Thus, especially reliable values of k_{ex}^h can be determined from cross-reactions with similarly small driving forces involving common coreactants having known self-exchange kinetics.²³ Suitable oxidants for this purpose are $\text{Co}(\text{en})_3^{3+}$, $\text{Ru}(\text{NH}_3)_6^{3+}$, and V_{aq}^{3+} . Careful inspection of Table II yields average values of k_{ex}^h for $\text{V}_{aq}^{3+/2+}$, $\text{Eu}_{aq}^{3+/2+}$, and $\text{Cr}_{aq}^{3+/2+}$ of ca. $5 (\pm 4) \times 10^{-2}$, $2 (\pm 1.5) \times 10^{-4}$, and $\sim 2 \times 10^{-6} \text{ M}^{-1} \text{ s}^{-1}$, respectively.

The estimation of k_{ex}^h for $\text{Ru}_{aq}^{3+/2+}$ self-exchange in the same manner is slightly less straightforward on account of the more positive formal potential for this couple (-20 mV vs. SCE; $\mu = 0.4$; Table I). Values of k_{ex}^h obtained from suitable cross-reactions ($f > 0.2$), involving V_{aq}^{2+} , $\text{Ru}(\text{NH}_3)_6^{2+}$, $\text{Co}(\text{phen})_3^{3+}$, $\text{Ru}(\text{NH}_3)_5\text{py}^{3+}$, and $\text{Ru}(\text{NH}_3)_5\text{isn}^{3+}$ as coreactants, vary by a factor of almost 200 (Table II). However, the relatively low value ($0.4 \text{ M}^{-1} \text{ s}^{-1}$) obtained with $\text{Co}(\text{phen})_3^{3+}$ is also characteristic of cross-reactions involving this oxidant with V_{aq}^{2+} , Eu_{aq}^{2+} , and Cr_{aq}^{2+} (Table II). Also, the estimate

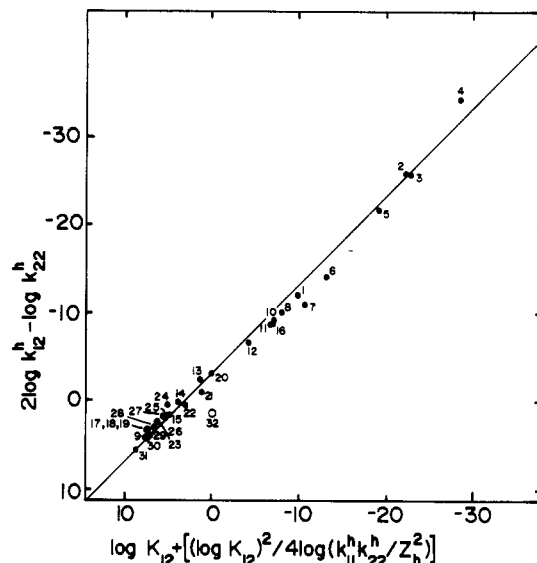


Figure 1. Plot of $(2 \log k_{12}^h - \log k_{22}^h)$ vs. $[\log K_{12} + (\log K_{12})^2 / 4 \log(k_{11}^h k_{22}^h / Z_h^2)]$ for homogeneous cross-reactions involving $\text{Fe}_{aq}^{3+/2+}$, calculated as Fe_{aq}^{2+} oxidations. k_{ex}^h for low-spin III/II polypyridines was taken as $1 \times 10^9 \text{ M}^{-1} \text{ s}^{-1}$ (see text). k_{11}^h refers to $\text{Fe}_{aq}^{3+/2+}$ self-exchange and k_{22}^h to self-exchange for coreactant couples. Z_h was assumed to equal $1 \times 10^{12} \text{ M}^{-1} \text{ s}^{-1}$; the value of k_{11}^h ($\sim 10^{-3} \text{ M}^{-1} \text{ s}^{-1}$) required for the plot was obtained by iteration. Data sources are given in Table II or ref 11 unless indicated otherwise. Closed points refer to cross-reactions; the open point refers to "observed" $\text{Fe}_{aq}^{3+/2+}$ self-exchange. Key to oxidants: (1) Ru_{aq}^{3+} ; (2) Eu_{aq}^{3+} ; (3) Cr_{aq}^{3+} ; (4) U_{aq}^{4+} ; (5) V_{aq}^{3+} ; (6) $\text{Ru}(\text{NH}_3)_6^{3+}$; (7) $\text{Ru}(\text{en})_3^{3+}$; (8) $\text{Ru}(\text{NH}_3)_5\text{py}^{3+}$; (9) $\text{Ru}(\text{bpy})_3^{3+}$; (10) $\text{Ru}(\text{NH}_3)_5\text{nic}^{3+}$; (11) $\text{Ru}(\text{NH}_3)_5\text{isn}^{3+}$; (12) $\text{Ru}(\text{NH}_3)_4\text{bpy}^{3+}$; (13) $\text{Os}(\text{bpy})_3^{3+}$; (14) $\text{Fe}(\text{bpy})_3^{3+}$; (15) $\text{Fe}(\text{phen})_3^{3+}$; (16) $\text{Co}(\text{phen})_3^{3+}$; (17) $\text{Ru}(\text{terpy})_2^{3+}$; (18) $\text{Ru}(\text{phen})_3^{3+}$; (19) $\text{Ru}(\text{bpy})_2(\text{py})_2^{3+}$; (20) $\text{Os}(5,5'-(\text{CH}_3)_2\text{bpy})_3^{3+}$; (21) $\text{Os}(\text{phen})_3^{3+}$; (22) $\text{Os}(5\text{-Cl-phen})_3^{3+}$; (23) $\text{Ru}(5,5'-(\text{CH}_3)_2\text{bpy})_3^{3+}$; (24) $\text{Ru}(3,4,7,8-(\text{CH}_3)_4\text{phen})_3^{3+}$; (25) $\text{Ru}(3,5,6,8-(\text{CH}_3)_4\text{phen})_3^{3+}$; (26) $\text{Ru}(4,7-(\text{CH}_3)_2\text{phen})_3^{3+}$; (27) $\text{Ru}(4,4'-(\text{CH}_3)_2\text{bpy})_3^{3+}$; (28) $\text{Ru}(5,6-(\text{CH}_3)_2\text{phen})_3^{3+}$; (29) $\text{Ru}(5-\text{CH}_3\text{phen})_3^{3+}$; (30) $\text{Ru}(5-\text{C}_6\text{H}_5\text{phen})_3^{3+}$; (31) $\text{Ru}(5\text{-Cl-phen})_3^{3+}$; (32) Fe_{aq}^{3+} .

of k_{ex}^h obtained from the $\text{Ru}_{aq}^{3+} - \text{V}_{aq}^{2+}$ reaction ($2 \text{ M}^{-1} \text{ s}^{-1}$) is likely to be too small since the free energy barrier for V_{aq}^{2+} oxidation appears to respond to changes in driving force to a noticeably smaller extent than predicted from eq 2.¹⁵ The remaining cross-reactions yield a reasonably consistent estimate of k_{ex}^h for $\text{Ru}_{aq}^{3+/2+}$ of ca. $50 (\pm 20) \text{ M}^{-1} \text{ s}^{-1}$. (A somewhat larger estimate of k_{ex}^h , ca. $200 \text{ M}^{-1} \text{ s}^{-1}$,²⁴ was arrived at previously from related arguments but involved extrapolation of values of k_{ex}^h obtained from cross-reactions having highly varying driving forces.²⁵)

The "observed" value of k_{ex}^h for $\text{V}_{aq}^{3+/2+}$, $3 \times 10^{-2} \text{ M}^{-1} \text{ s}^{-1}$ (i.e., that obtained directly from the observed self-exchange kinetics), is close to the estimates obtained from cross-reactions with $\text{Co}(\text{en})_3^{3+}$ and $\text{Ru}(\text{NH}_3)_6^{3+}$. In contrast, the "observed" value of k_{ex}^h for $\text{Fe}_{aq}^{3+/2+}$, $15 \text{ M}^{-1} \text{ s}^{-1}$, is considerably (10^3 - to 10^5 -fold) larger than those derived from cross-reactions having suitably small driving forces ($f \geq 0.2$) (Table II). Equation 2 can be rewritten as

$$\log k_{12}^h = 0.5(\log k_{11}^h + \log k_{22}^h) + 0.5 \log K_{12} + \frac{(\log K_{12})^2}{8 \log(k_{11}^h k_{22}^h / A_h^2)} \quad (9)$$

(20) E. L. Yee, R. J. Cave, K. L. Guyer, P. D. Tyma, and M. J. Weaver, *J. Am. Chem. Soc.*, **101**, 1131 (1979).

(21) E. L. Yee and M. J. Weaver, *Inorg. Chem.*, **19**, 1077 (1980).

(22) R. C. Young, F. R. Keene, and T. J. Meyer, *J. Am. Chem. Soc.*, **99**, 2468 (1977).

(23) Under these conditions it is likely that any residual work terms will affect each value of k_{ex}^h to an essentially equal extent. In addition, the predominant reaction channel for cross-reactions having similarly small driving forces will involve transition-state structures that closely resemble those for the parent self-exchange reactions.¹⁵

(24) The estimate of k_{ex}^h , $60 \text{ M}^{-1} \text{ s}^{-1}$, for $\text{Ru}_{aq}^{3+/2+}$ given in ref 25 refers to an ionic strength of 1 M and is therefore uncorrected for work terms. Application of this correction yields $k_{ex}^h \approx 200 \text{ M}^{-1} \text{ s}^{-1}$.

(25) W. Botcher, G. M. Brown, and N. Sutin, *Inorg. Chem.*, **18**, 1447 (1979).

Table III. Summary of Rate Constants for Electron Exchange at 25 °C and Comparison with Theoretical Predictions

redox couple	$k_{\text{ex}}^e, {}^a \text{ cm s}^{-1}$	$k_{\text{ex}}^h, {}^b \text{ M}^{-1} \text{ s}^{-1}$	$k_{\text{ex}}^h(\text{eq 7}), {}^c \text{ M}^{-1} \text{ s}^{-1}$	$k_{\text{ex}}^h(\text{calcd}), {}^d \text{ M}^{-1} \text{ s}^{-1}$	$\Delta S_{\text{rc}}^{\circ}, {}^e \text{ cal deg}^{-1} \text{ mol}^{-1}$
$\text{Ru}_{\text{aq}}^{3+/2+}$	2×10^{-2}	50 (1)	25 (1)	2.5×10^5 (1)	36
$\text{V}_{\text{aq}}^{3+/2+}$	1×10^{-3}	5×10^{-2} , [3×10^{-2}] (1×10^{-3}), (6×10^{-4})	6×10^{-2} (2.5×10^{-3})		37
$\text{Fe}_{\text{aq}}^{3+/2+}$	$\lesssim 1 \times 10^{-4}$	$\sim 1 \times 10^{-3}$, [15] ($\sim 2 \times 10^{-5}$), (0.3)	$\lesssim 6 \times 10^{-4}$ ($\sim 3 \times 10^{-5}$)	90 (3.5×10^{-4})	43
$\text{Eu}_{\text{aq}}^{3+/2+}$	8×10^{-5}	2×10^{-4} (4×10^{-6})	4×10^{-4} (1.5×10^{-5})		48
$\text{Cr}_{\text{aq}}^{3+/2+}$	2×10^{-6}	2×10^{-6} (4×10^{-8})	2.5×10^{-6} (1×10^{-8})	1×10^{-4} (4×10^{-10})	49

^a Work-corrected rate constant for electrochemical exchange at the mercury-aqueous interface; from Table I. ^b Average work-corrected rate constant for homogeneous self-exchange; determined from cross-reaction data (Table II) by using eq 2 (see text). Values for $\text{V}_{\text{aq}}^{3+/2+}$ and $\text{Fe}_{\text{aq}}^{3+/2+}$ in brackets were obtained "directly" from self-exchange kinetics. Values in parentheses underneath are ratios of k_{ex}^h with respect to that for $\text{Ru}_{\text{aq}}^{3+/2+}$. ^c Estimates of k_{ex}^h from corresponding values of k_{ex}^e and eq 7, assuming that $A_{\text{h}} = 3.5 \times 10^{12} \text{ M}^{-1} \text{ s}^{-1}$. $A_{\text{e}} = 1 \times 10^5 \text{ cm s}^{-1}$, and $C = 3.0 \text{ kcal mol}^{-1}$ (see text). Values in parentheses underneath are ratios of $k_{\text{ex}}^h(\text{eq 7})$ with respect to that for $\text{Ru}_{\text{aq}}^{3+/2+}$. ^d Values of k_{ex}^h calculated from eq 3, with the assumption that $\kappa = 1$, $A_{\text{h}} = 3.5 \times 10^{12} \text{ M}^{-1} \text{ s}^{-1}$, and $\Delta G_{\text{ex}}^* = \Delta G_{\text{is}}^* + \Delta G_{\text{os}}^*$, where ΔG_{is}^* and ΔG_{os}^* were obtained from eq 11 and 5a, respectively (see text). Values in parentheses underneath are ratios of $k_{\text{ex}}^h(\text{calcd})$ with respect to that for $\text{Ru}_{\text{aq}}^{3+/2+}$. ^e Reaction entropy for redox couple, determined at ionic strength $\mu \approx 0.5$; values taken from ref 20.

Therefore, a plot of $(2 \log k_{12}^h - \log k_{22}^h)$ vs. $[\log K_{12} + (\log K_{12})^2 / [4 \log (k_{11}^h k_{22}^h / Z_h^2)]]$ should yield a straight line of slope 1.0 with an intercept equal to $\log k_{11}^h$.²⁶ Figure 1 shows such a plot for 32 reactions involving $\text{Fe}_{\text{aq}}^{3+/2+}$, formally expressed as $\text{Fe}_{\text{aq}}^{2+}$ oxidations. (The data sources are indicated by footnote citations; A_{h} is assumed to equal $1 \times 10^{12} \text{ M}^{-1} \text{ s}^{-1}$. The value of k_{11}^h in the last term in eq 9 was obtained by iteration; for most reactions choosing any reasonable value of k_{11}^h in the range ca. 10^{-4} – $10 \text{ M}^{-1} \text{ s}^{-1}$ led to essentially identical results.) The straight line of slope 1.0 in Figure 1 provides the best fit to the solid points, which refer to the cross-reactions. The intercept, which equals $\log k_{\text{ex}}^h$ for $\text{Fe}_{\text{aq}}^{3+/2+}$, corresponds to $k_{\text{ex}}^h = 7 \times 10^{-4} \text{ M}^{-1} \text{ s}^{-1}$. The open point, which refers to the "observed" value of k_{ex}^h ($15 \text{ M}^{-1} \text{ s}^{-1}$), is clearly at variance with the other points, yielding a discrepancy of over 10^4 -fold in k_{ex}^h . Figure 2 shows a similar plot for cross-reactions involving $\text{V}_{\text{aq}}^{3+/2+}$. Although the data points are less numerous, the open point for $\text{V}_{\text{aq}}^{3+/2+}$ self-exchange ($k_{\text{ex}}^h = 3 \times 10^{-2} \text{ M}^{-1} \text{ s}^{-1}$) is consistent with the remaining entries. Admittedly, the slope (0.9) of the best fit line in Figure 2 differs somewhat from unity; possible causes are discussed elsewhere.¹⁵

Such a behavioral difference between $\text{V}_{\text{aq}}^{3+/2+}$ and $\text{Fe}_{\text{aq}}^{3+/2+}$ has been noted previously.¹⁰ The striking discrepancies with eq 2 for $\text{Fe}_{\text{aq}}^{3+/2+}$ were ascribed in part to especially facile reaction pathways for self-exchange of the cross-reaction partners that contain pyridine-type ligands arising from interpenetration of the pyridine rings. Since such interactions will be absent for the $\text{Fe}_{\text{aq}}^{3+/2+}$ cross-reactions, the resulting estimates of k_{ex}^h for $\text{Fe}_{\text{aq}}^{3+/2+}$ (ca. 10^{-4} – 10^{-3} M s^{-1}) were considered to be falsely small, the observed self-exchange rate constant being presumed to reflect a "normal" outer-sphere pathway.¹⁰

A difficulty in comparing data for cross-reactions involving $\text{Fe}_{\text{aq}}^{3+/2+}$ with the other aquo couples is that the formal potential for $\text{Fe}_{\text{aq}}^{3+/2+}$ is substantially more positive of those for the remaining aquo couples. Therefore, cross-reactions having suitably small driving forces inevitably involve different co-reactants with the likelihood that systematic errors in the applicability of eq 2 could occur. These errors could vitiate its use for obtaining even relative values of the self-exchange kinetics of $\text{Fe}_{\text{aq}}^{3+/2+}$ with respect to the other couples. However, the comparison of the kinetics of the $\text{Os}(\text{bpy})_3^{3+}$ – $\text{Fe}_{\text{aq}}^{2+}$

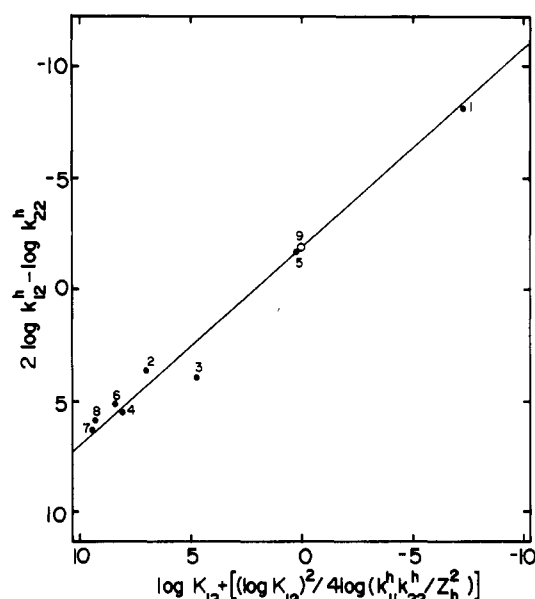


Figure 2. As for Figure 1 but for cross-reactions involving $\text{V}_{\text{aq}}^{3+/2+}$, expressed as $\text{V}_{\text{aq}}^{2+}$ oxidations. k_{11}^h refers to $\text{V}_{\text{aq}}^{3+/2+}$ self-exchange. Data sources are from Table II or ref 11 unless indicated otherwise. Key to oxidants: (1) $\text{U}_{\text{aq}}^{4+}$; (2) $\text{Ru}_{\text{aq}}^{3+}$; (3) $\text{Ru}(\text{NH}_3)_6^{3+}$; (4) $\text{Ru}(\text{NH}_3)_5\text{py}^{3+}$; (5) $\text{Co}(\text{en})_3^{3+}$; (6) $\text{Co}(\text{bpy})_3^{3+}$; (7) $\text{Ru}(\text{NH}_3)_5\text{sisn}^{3+}$; (8) $\text{Co}(\text{phen})_3^{3+}$; (9) $\text{V}_{\text{aq}}^{3+}$.

and $\text{V}_{\text{aq}}^{3+}$ – $\text{Cr}(\text{bpy})_3^{2+}$ cross-reactions provides a way of circumventing this problem. Both these reactions have suitably small driving forces [equilibrium constants of 80 and 1.2, respectively (Table II)], and the coreacting redox couples, $\text{Os}(\text{bpy})_3^{3+/2+}$ and $\text{Cr}(\text{bpy})_3^{3+/2+}$, not only have the same ligand composition but also are likely to have similarly small barriers to electron exchange since they both involve electron acceptance into a delocalized t_{2g} orbital.¹⁰ Therefore, on the assumptions that the rate constants for $\text{Os}(\text{bpy})_3^{3+/2+}$ and $\text{Cr}(\text{bpy})_3^{3+/2+}$ self-exchange, k_{22} and k_{44} , are equal and that the f terms are essentially unity, the ratio of the rate constants for $\text{Fe}_{\text{aq}}^{3+/2+}$ and $\text{V}_{\text{aq}}^{3+/2+}$ self-exchange, $k_{\text{ex,Fe}}^h/k_{\text{ex,V}}^h$, can be found from the kinetics and thermodynamic data for the corresponding cross-reaction by using (cf. eq 2)

$$k_{\text{ex,Fe}}^h/k_{\text{ex,V}}^h (\equiv k_{11}/k_{33}) = k_{12}^2 k_{44} K_{34} / k_{34}^2 k_{22} K_{12} \quad (10)$$

Inserting the experimental values $k_{12} = 3 \times 10^3$, $k_{34} = 1 \times 10^3 \text{ M}^{-1} \text{ s}^{-1}$, $K_{12} = 80$, and $K_{34} = 1.2$ (Table II) into eq 10 yields $k_{\text{ex,Fe}}^h/k_{\text{ex,V}}^h = 0.14$. Taking $k_{\text{ex,V}}^h$ to be $5 \times 10^{-2} \text{ M}^{-1} \text{ s}^{-1}$ (vide supra) yields the result $k_{\text{ex,Fe}}^h = 7 \times 10^{-3} \text{ M}^{-1} \text{ s}^{-1}$.²⁸

(26) J. F. Endicott, B. Durham, and K. Kumar, *Inorg. Chem.*, **21**, 2437 (1982).

(27) G. M. Brown, H. J. Krentzien, M. Abe, and H. Taube, *Inorg. Chem.*, **18**, 3374 (1979).

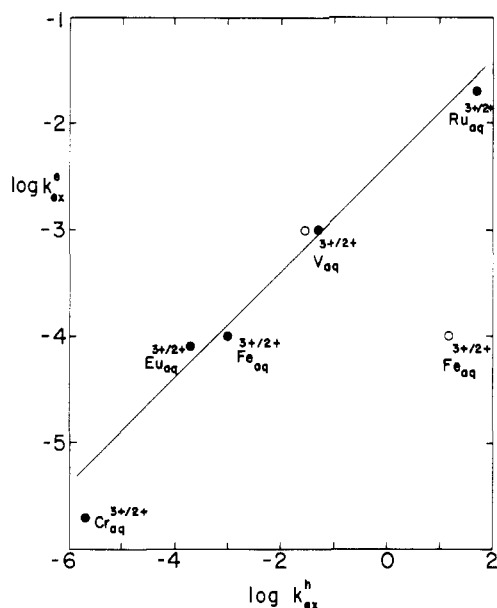


Figure 3. Comparison of rate constants for electrochemical exchange at the mercury–aqueous interface, k_{ex}^e (cm s⁻¹), with corresponding rate constants for homogeneous self-exchange, k_{ex}^h (M⁻¹ s⁻¹), taken from Table III. Closed points refer to values of k_{ex}^h obtained from homogeneous cross-reactions; open points, to those obtained from measured self-exchange kinetics. The straight line is the relationship between $\log k_{\text{ex}}^e$ and $\log k_{\text{ex}}^h$ expected from eq 7.

This value of k_{ex}^h for $\text{Fe}_{\text{aq}}^{3+/2+}$ is again over 10³-fold smaller than that obtained from the self-exchange kinetics.

Comparison between Electrochemical and Homogeneous Exchange Kinetics

Strong evidence supporting the validity of such smaller estimates of k_{ex}^h is obtained from the rate constants for electrochemical exchange, k_{ex}^e . Table III contains a summary of the “best fit” values of k_{ex}^e and k_{ex}^h for each redox couple, along with estimates of k_{ex}^h , k_{ex}^h (eq 7), obtained from the corresponding values of k_{ex}^e by using eq 7. The values given in parentheses are ratios of k_{ex}^h and k_{ex}^h (eq 7) with respect to those for $\text{Ru}_{\text{aq}}^{3+/2+}$ ($k_{\text{ex}}^h/k_{\text{ex,Ru}}^h$). The frequency factors A_h and A_e required in eq 7 were estimated from an “encounter preequilibrium” model^{1,29–33} using the expressions $A_h = 4\pi N r_h^2 (\delta r_h) \nu_n / 10^3$ and $A_e = (\delta r_e) \nu_n$,³² where N is Avogadro’s number, r_h is the average distance between the homogeneous redox centers in the transition state, δr_h is the approximate range of encounter distances (“reaction zone thickness”) within which electron transfer occurs, δr_e is the corresponding reaction zone thickness close to the electrode surface, and ν_n is the effective nuclear activation frequency.¹ Inserting the anticipated values $r_h = 7 \text{ \AA}$, $\delta r_h = \delta r_e \approx 1 \text{ \AA}$,^{30,32} and $\nu_n = 1 \times 10^{13} \text{ s}^{-1}$,³⁰ for the present aquo couples into these expressions yields $A_h = 3.5 \times 10^{12} \text{ M}^{-1} \text{ s}^{-1}$ and $A_e = 1 \times 10^5 \text{ cm s}^{-1}$. The value

of C in eq 7 was estimated to be 3.0 kcal mol⁻¹ by inserting the values $R_h = 7 \text{ \AA}$ and $R_e = 13 \text{ \AA}$ ³⁴ into eq 6. (Note that, although there is some uncertainty in the appropriate absolute values of both R_h and R_e , this partially cancels in eq 6.)

The absolute as well as relative values of k_{ex}^h (eq 7) are seen to be uniformly in good agreement with those values of k_{ex}^h (eq 7) obtained from homogeneous cross reactions. This is also illustrated in Figure 3 as a plot of $\log k_{\text{ex}}^e$ against $\log k_{\text{ex}}^h$. The straight line represents the correlation predicted from eq 7. The solid points refer to values of k_{ex}^h obtained from cross reactions, and the open circles represent the values of k_{ex}^h for $\text{V}_{\text{aq}}^{3+/2+}$ and $\text{Fe}_{\text{aq}}^{3+/2+}$ obtained from the self-exchange kinetics. Although all the other entries are consistent with this correlation, that obtained from the $\text{Fe}_{\text{aq}}^{3+/2+}$ self-exchange kinetics is again about 10⁴-fold larger than expected.

Correlation of Intrinsic Barriers with Reactant Structure

As noted above, it is instructive to compare the variations in the experimental values of k_{ex}^h and k_{ex}^e with the structural properties of the redox couples. To a certain extent, the observed reactivity sequence $\text{Ru}_{\text{aq}}^{3+/2+} > \text{V}_{\text{aq}}^{3+/2+} > \text{Fe}_{\text{aq}}^{3+/2+} \gtrsim \text{Eu}_{\text{aq}}^{3+/2+} > \text{Cr}_{\text{aq}}^{3+/2+}$ is consistent with structural expectations; the three most reactive couples all involve the acceptance of the transferring electron into a t_{2g} orbital for which the required distortions of the metal–ligand geometry, and hence ΔG_{is}^* , are anticipated to be relatively small.⁷

The calculation of ΔG_{is}^* and hence k_{ex}^h or k_{ex}^e from electron-transfer theory requires quantitative information on the changes in the metal–ligand bond distances, Δa , accompanying electron transfer.^{1,9} Although sufficiently reliable determinations of Δa are sparse, recent X-ray diffraction measurements have established values for $\text{Ru}(\text{OH}_2)_6^{3+/2+}$ and $\text{Fe}(\text{OH}_2)_6^{3+/2+}$ of 0.09,³⁵ and 0.14 Å ,³⁶ respectively. An effective value of Δa for $\text{Cr}(\text{OH}_2)_6^{3+/2+}$, equal to 0.20 Å , has also been determined from solution EXAFS measurements.³⁰ The relation¹

$$\Delta G_{\text{is}}^* = n f_2 f_3 (\Delta a)^2 / 2(f_2 + f_3) \quad (11)$$

where n is the number of metal–ligand bonds involved (6) and f_2 and f_3 are the metal–ligand force constants in the divalent and trivalent oxidation states, with the corresponding metal–oxygen stretching frequencies assumed to be 390 and 490 cm⁻¹, respectively,¹ yields values of ΔG_{is}^* of 3.5, 8.4, and 17.2 kcal mol⁻¹ for $\text{Ru}_{\text{aq}}^{3+/2+}$, $\text{Fe}_{\text{aq}}^{3+/2+}$, and $\text{Cr}_{\text{aq}}^{3+/2+}$, respectively. Errors in these values may arise both from anharmonicity of the potential energy surfaces as well as from uncertainties in the appropriate force constants. The effective values of ΔG_{is}^* are slightly smaller as a result of nuclear tunneling;¹ the nuclear tunneling factors, Γ_n , of 1.5, 2, and 6 for $\text{Ru}_{\text{aq}}^{3+/2+}$, $\text{Fe}_{\text{aq}}^{3+/2+}$, and $\text{Cr}_{\text{aq}}^{3+/2+}$, respectively,^{1,30} yield effective values of ΔG_{is}^* equal to 3.25, 8.0, and 16.1 kcal mol⁻¹, respectively. The outer-shell contribution to ΔG_{ex}^* , ΔG_{os}^* , can be estimated from eq 5a; again, using the values $a = 3.5$ and $R_h = 7 \text{ \AA}$ yields $\Delta G_{\text{os}}^* = 6.5 \text{ kcal mol}^{-1}$. Inserting the resulting estimates of ΔG_{ex}^* into eq 3 along with the above estimate of A_h , $3.5 \times 10^{12} \text{ M}^{-1} \text{ s}^{-1}$, and assuming that $\kappa = 1$ yield the calculated values of k_{ex}^h , k_{ex}^h (calcd), listed in Table III. Ratios of k_{ex}^h (calcd) with respect to that for $\text{Ru}_{\text{aq}}^{3+/2+}$, ($k_{\text{ex}}^h/k_{\text{ex,Ru}}^h$)_{calcd} are also listed in parentheses in Table III alongside the corresponding experimental rate ratios.

(28) Admittedly, the self-exchange rates for $\text{Os}(\text{bpy})_3^{3+/2+}$ and $\text{Cr}(\text{bpy})_3^{3+/2+}$ may differ somewhat. However, if anything, the former reaction should have faster self-exchange kinetics as a result of greater delocalization of the transferred electron, which would yield an even smaller value of $k_{\text{ex,Fe}}^h$ from eq 7.

(29) G. M. Brown and N. Sutin, *J. Am. Chem. Soc.*, **101**, 883 (1979).

(30) B. S. Brunschwig, C. Creutz, D. H. Macartney, T.-K. Sham, and N. Sutin, *Faraday Discuss. Chem. Soc.*, **74**, 113 (1982).

(31) R. A. Marcus, *Int. J. Chem. Kinet.*, **13**, 865 (1981).

(32) J. T. Hupp and M. J. Weaver, *J. Electroanal. Chem. Interfacial Electrochem.*, in press.

(33) Although a frequency factor formulation based on the simple gas-phase collision model has conventionally been employed to estimate A_h and A_e ,⁹ the use of an “encounter preequilibrium” model where activation is considered to occur chiefly via unimolecular activation within a statistical distribution of encounter complexes appears to be physically more appropriate for both homogeneous^{29–31} and electrochemical³² electron-transfer processes.

(34) Since it is likely that the outer-sphere transition state for electrochemical reactions is separated from the electrode by a layer of water molecules,¹² R_e is estimated to be twice the sum of the reactant radius ($\sim 3.5 \text{ \AA}$) and the effective diameter of a water molecule (3 Å).

(35) P. Bernhard, H.-B. Burgi, J. Hauser, H. Lehmann, and A. Ludi, *Inorg. Chem.*, **21** 3936 (1982).

(36) N. J. Hair and J. K. Beattie, *Inorg. Chem.*, **16**, 245 (1977); J. K. Beattie, S. P. Best, B. W. Skelton, and A. H. White, *J. Chem. Soc., Dalton Trans.*, 2105 (1981).

For all three couples it is seen that $k_{\text{ex}}^{\text{h}} < k_{\text{ex}}^{\text{h}}(\text{calcd})$, the calculated values being about 3–4 orders of magnitude larger than both k_{ex}^{h} and $k_{\text{ex}}^{\text{h}}(\text{eq 7})$. The “observed” value of k_{ex}^{h} for $\text{Fe}_{\text{aq}}^{3+/2+}$ self-exchange, $k_{\text{ex,Fe}}^{\text{h}}$, is substantially closer to $k_{\text{ex,Fe}}^{\text{h}}(\text{calcd})$, which might be viewed as evidence that this value corresponds more closely to the “true” intrinsic barrier for $\text{Fe}_{\text{aq}}^{3+/2+}$.³⁰ However, the overriding evidence suggests otherwise. Thus, the calculated rate ratio, $(k_{\text{ex,Fe}}^{\text{h}}/k_{\text{ex,Ru}}^{\text{h}})$, for the $\text{Fe}_{\text{aq}}^{3+/2+}$ vs. $\text{Ru}_{\text{aq}}^{3+/2+}$ couples (3.5×10^{-4}) is roughly comparable to the corresponding experimental rate ratio obtained from cross-reactions ($\sim 2 \times 10^{-5}$) and electrochemical reactivities ($\sim 3 \times 10^{-5}$) but substantially smaller than that obtained by using the “observed” value of $k_{\text{ex,Fe}}^{\text{h}}$ (0.3) (Table III).

Recent calculations suggest that the $\text{Fe}_{\text{aq}}^{3+/2+}$ self-exchange reaction is significantly nonadiabatic ($\kappa \approx 0.01$) at the normal ion–ion “contact” distance of 6.9 Å,^{2,37} although some overlap of the reactant cospheres seems feasible.^{37,38} Since the values of κ will depend upon the extent of electronic coupling with the coreactants, and hence upon the electronic and ligand structures, such nonadiabaticity ($\kappa \ll 1$) may account for some disparities in k_{ex}^{h} obtained with different coreactants, for example, the low values obtained here by using $\text{Co}(\text{phen})_3^{3+/2+}$ (vide supra). Nevertheless, although nonadiabatic effects could account in part for the discrepancies between k_{ex}^{h} and $k_{\text{ex}}^{\text{h}}(\text{calcd})$, their inclusion is unlikely to increase the ratio $(k_{\text{ex,Fe}}^{\text{h}}/k_{\text{ex,Ru}}^{\text{h}})_{\text{calcd}}$ since the 4d ruthenium orbitals are more likely to couple effectively than the more compact 3d iron orbitals, thereby yielding larger κ values for the $\text{Ru}_{\text{aq}}^{3+/2+}$ reactions. Consequently, the rate ratio $k_{\text{ex,Fe}}^{\text{h}}/k_{\text{ex,Ru}}^{\text{h}}$ (0.3) obtained from the $\text{Fe}_{\text{aq}}^{3+/2+}$ self-exchange kinetics is not consistent with these theoretical expectations.

It might be argued that the discrepancies $k_{\text{ex}}^{\text{h}}(\text{eq 7}) < k_{\text{ex}}^{\text{h}}(\text{calcd})$ arise at least in part from nonadiabaticity of the electrochemical reactions, especially since current physical models of the double layer suggest that the reactant–electrode distance at the plane of closest approach may be approximately the same as the distance separating the reacting pair in homogeneous outer-sphere reactions.^{12,39,40} Although such reactions may be marginally nonadiabatic, it is unlikely that they are especially so. Thus, the frequency factors determined from the temperature dependence of rate constants at mercury are not especially anomalous.^{15,41} The $\text{Cr}_{\text{aq}}^{3+/2+}$ electrochemical exchange reaction at mercury has been ascertained to be only marginally nonadiabatic, $\kappa \approx 0.2$ – 0.5 , from a comparison with the rates of closely related inner-sphere electrode reactions.⁵⁸ Even if the electrochemical as well as the homogeneous reactions are indeed nonadiabatic, the κ values would appear to be roughly (to within, e.g., a factor of 10) independent of a reaction environment for each redox couple in order to account for the consistently good agreement with the predictions of eq 2 and 7. Since κ is expected to be sensitive to the nature of the donor and acceptor orbitals in each reactant pair, this implies that κ is unlikely to lie below ca. 10^{-3} , especially in view of the variety of orbital symmetries (t_{2g} , e_g , f) involved in the present systems.⁸

A major reason for the observed discrepancies between k_{ex}^{h} and $k_{\text{ex}}^{\text{h}}(\text{calcd})$ could arise from a deficiency in the theoretical models used to calculate ΔG_{ex}^* and/or the work terms. In addition to the possible errors in the calculated values of ΔG_{is}^* noted above, the outer-shell barrier ΔG_{os}^* could be larger than calculated from eq 5 in both homogeneous and electrochemical

environments as a result of alterations in short-range solvent polarization that are known to accompany electron transfer.^{14,20,42,43}

Finally, it is instructive to compare the relative values of k_{ex}^{h} and k_{ex}^{e} with the reaction entropies $\Delta S_{\text{rc}}^{\circ}$ for the redox couples (Table III).²⁰ The latter values provide a monitor of the changes in solvent polarization that accompany formation of $\text{M}_{\text{aq}}^{2+}$ from $\text{M}_{\text{aq}}^{3+}$. The magnitude of $\Delta S_{\text{rc}}^{\circ}$ might be expected to parallel ΔG_{is}^* and hence ΔG_{ex}^* ,⁴⁴ larger values of Δa should yield greater alterations in the electron density of the aquo hydrogens⁴⁵ and hence more extensive changes in the extent of ligand–solvent hydrogen bonding induced by electron transfer. Indeed, the observed sequence of $\Delta S_{\text{rc}}^{\circ}$ values $\text{Ru}_{\text{aq}}^{3+/2+} < \text{V}_{\text{aq}}^{3+/2+} < \text{Fe}_{\text{aq}}^{3+/2+} < \text{Eu}_{\text{aq}}^{3+/2+} < \text{Cr}_{\text{aq}}^{3+/2+}$ uniformly parallels the observed reactivity sequence (Table III) although yet again the value of k_{ex}^{h} for $\text{Fe}_{\text{aq}}^{3+/2+}$ obtained from self-exchange data is not consistent with this trend.

Conclusions and Mechanistic Implications

Taken together, the above results provide strong support to the suspicions noted previously^{46,47} that the intrinsic barrier to outer-sphere electron exchange for $\text{Fe}_{\text{aq}}^{3+/2+}$ is significantly greater than anticipated from the measured self-exchange kinetics. Persuasive evidence is provided by the observation that the electrochemical reactivity of $\text{Fe}_{\text{aq}}^{3+/2+}$ is noticeably smaller than that of $\text{Ru}_{\text{aq}}^{3+/2+}$ and even $\text{V}_{\text{aq}}^{3+/2+}$ under the same or comparable conditions at the mercury–aqueous interface and by the uniformly good agreement between k_{ex}^{h} (eq 7) and the values of k_{ex}^{h} extracted from homogeneous cross-reactions having suitably small driving forces and structurally similar coreactants. On this basis, the reported self-exchange rate constant for $\text{Fe}_{\text{aq}}^{3+/2+}$ may well be at least 10^3 -fold larger than that corresponding to the “normal” outer-sphere intrinsic barrier for this couple in other homogeneous and also electrochemical environments.

It remains to consider physical reasons for the enhanced reactivity of the $\text{Fe}_{\text{aq}}^{3+/2+}$ couple when undergoing self-exchange. One possibility is that the “observed” value of k_{ex}^{h} refers to a “normal” outer-sphere pathway, the electrochemical and homogeneous cross-reaction data corresponding to “abnormal”, for example strongly nonadiabatic, pathways that are all less favorable by about 10^3 - to 10^5 -fold in k_{ex}^{h} . While not beyond the bounds of possibility, the weight of evidence presented above would seem to strongly disfavor this explanation. A more likely possibility is that the self-exchange reaction proceeds via a more facile inner-sphere pathway. Although the presence of an acid-independent pathway for $\text{Fe}_{\text{aq}}^{3+/2+}$ self-exchange has recently been confirmed by using mixed LiClO_4 – HClO_4 electrolytes,³⁰ this result by no means eliminates the possibility that the observed pathway involves a water-bridged inner-sphere transition state. The observed acid-independent rate constant for $\text{Co}_{\text{aq}}^{3+/2+}$ self-exchange has recently been demonstrated to be ca. 10^{12} -fold larger than that obtained from cross-reaction data and attributed to the presence of a water-bridged pathway.²⁶ It was suggested that the dominant presence of such pathways may be confined to redox couples such as $\text{Co}_{\text{aq}}^{3+/2+}$ with extremely positive standard potentials on the basis of a model where the inner-sphere reaction coordinate involves metal-bridging ligand homolysis.^{26,48} Such a pathway would, all other factors being

(37) M. D. Newton, *ACS Symp. Ser.*, No. 198, 255 (1982).

(38) B. L. Tempe, H. L. Friedman, and M. D. Newton, *J. Chem. Phys.*, **76**, 1490 (1982).

(39) M. J. Weaver and T. L. Satterberg, *J. Phys. Chem.*, **81**, 1772 (1977).

(40) M. J. Weaver, H. Y. Liu, and Y. Kim, *Can. J. Chem.*, **59**, 1944 (1981).

(41) M. J. Weaver, *J. Phys. Chem.*, **83**, 1748 (1979); *Isr. J. Chem.*, **18**, 35 (1979).

(42) M. J. Weaver and S. M. Nettles, *Inorg. Chem.*, **19**, 1641 (1980).

(43) J. T. Hupp and M. J. Weaver, to be submitted for publication.

(44) N. Sutin, M. J. Weaver, and E. L. Yee, *Inorg. Chem.*, **19**, 1096 (1980).

(45) J. A. Jafri, J. Logan, and M. D. Newton, *Isr. J. Chem.*, **19**, 340 (1980).

(46) T. D. Hand, M. R. Hyde, and A. G. Sykes, *Inorg. Chem.*, **14**, 1720 (1975).

(47) J. N. Braddock and T. J. Meyer, *J. Am. Chem. Soc.*, **95**, 3158 (1973).

(48) J. F. Endicott, C.-L. Wong, J. M. Ciskowski, and K. P. Balakrishnan, *J. Am. Chem. Soc.*, **102**, 2100 (1980).

equal, be less favorable for $\text{Fe}_{\text{aq}}^{3+/2+}$ self-exchange since $\text{Fe}_{\text{aq}}^{3+}$ is a considerably less strong oxidant than $\text{Co}_{\text{aq}}^{3+}$.²⁶ However, this could easily be offset by the manifold other factors that control the relative rates of competing inner- and outer-sphere pathways.⁴⁹ In any case, on this basis water bridging is more likely for $\text{Fe}_{\text{aq}}^{3+/2+}$ self-exchange than for the other aquo complexes considered here;⁵⁰ aside from $\text{Ru}_{\text{aq}}^{3+/2+}$, which is constrained to follow outer-sphere pathways, all the other couples considered here are ca. 1 V less strongly oxidizing than $\text{Fe}_{\text{aq}}^{3+/2+}$. Such pathways are clearly unavailable for cross-reactions involving substitutionally inert coreactants such as those in Table II, so that the $\text{Fe}_{\text{aq}}^{3+/2+}$ reactivity within these environments should reflect that for a "normal" outer-sphere pathway. Water- or hydroxo-bridged pathways are also unlikely within electrochemical redox environments, especially at mercury electrodes in view of the weak interaction between water molecules and this surface.⁵¹

(49) Footnote 54 of ref 26.

(50) It was asserted⁴⁹ that the $\text{Co}_{\text{aq}}^{3+}$ - $\text{Fe}_{\text{aq}}^{2+}$ reaction follows an outer-sphere pathway on the basis of the agreement with the rates of other cross-reactions involving $\text{Co}_{\text{aq}}^{3+}$ and outer-sphere reductants calculated by using eq 2 and the measured value of $k_{\text{ex}}^{\text{Fe}}$. However, using the present estimate of $k_{\text{ex}}^{\text{Fe}}$ for outer-sphere $\text{Fe}_{\text{aq}}^{3+/2+}$ self-exchange instead yields a $\text{Co}_{\text{aq}}^{3+}$ - $\text{Fe}_{\text{aq}}^{2+}$ reaction rate ca. 10^3 -fold larger than predicted from eq 2, indicative of a water-bridged pathway for this reaction as well.

(51) For example, see S. Trassati, *J. Electroanal. Chem. Interfacial Electrochem.*, **123**, 121 (1981).

Regardless of the detailed reasons for the anomalous behavior of $\text{Fe}_{\text{aq}}^{3+/2+}$ self-exchange it can be concluded that this couple is in some respects a nonideal choice for the detailed comparisons between experimental rate parameters and the predictions of contemporary theory.¹ Nevertheless, the required structural information is becoming available for a number of other redox couples,³⁰ enabling such comparisons to be made not only for self-exchange reactions³⁰ but also for a variety of cross-reactions and electrochemical processes.⁴³

Acknowledgment. We are grateful to Dr. A. Ludi for communicating his results on ruthenium aquo crystal structures in advance of publication. This work is supported by the Air Force Office of Scientific Research.

Registry No. Ru, 7440-18-8; V, 7440-62-2; Fe, 7439-89-6; Eu, 7440-53-1; Cr, 7440-47-3.

(52) B. M. Gordon, L. L. Williams, and N. Sutin, *J. Am. Chem. Soc.*, **83**, 2061 (1961).

(53) M. H. Ford-Smith and N. Sutin, *J. Am. Chem. Soc.*, **83**, 1830 (1961).

(54) N. Sutin and B. M. Gordon, *J. Am. Chem. Soc.*, **83**, 70 (1961).

(55) T. J. Przystas and N. Sutin, *J. Am. Chem. Soc.*, **95**, 5545 (1973).

(56) Y. Ohsawa, T. Sajiand, and S. Aoyagui, *J. Electroanal. Chem. Interfacial Electrochem.*, **106**, 327 (1980).

(57) C. T. Lin, W. Böttcher, M. Chou, C. Creutz, and N. Sutin, *J. Am. Chem. Soc.*, **98**, 6536 (1976).

(58) J. T. Hupp and M. J. Weaver, submitted for publication.

Contribution from the Laboratory of Analytical Chemistry, Faculty of Science, Nagoya University, Nagoya 464, Japan

Activation Volume as Evidence for a Dissociative-Interchange Mechanism of Nickel(II) Ion Complexation with Isoquinoline in Water, *N,N*-Dimethylformamide, Acetonitrile, Methanol, and Ethanol

KOJI ISHIHARA, SHIGENOBU FUNAHASHI, and MOTOHARU TANAKA*

Received January 14, 1983

Activation volumes for the complexation of nickel(II) ion with isoquinoline in various solvents were determined by a high-pressure stopped-flow technique. Values of activation volume for formation and dissociation of the (isoquinoline)nickel(II) complex are respectively 7.4 ± 1.3 and 8.9 ± 0.8 $\text{cm}^3 \text{mol}^{-1}$ in water, 9.3 ± 0.3 and 12.2 ± 0.3 $\text{cm}^3 \text{mol}^{-1}$ in *N,N*-dimethylformamide, 12.8 ± 0.6 and 9.9 ± 0.5 $\text{cm}^3 \text{mol}^{-1}$ in methanol, and 12.6 ± 0.5 and 15.7 ± 1.1 $\text{cm}^3 \text{mol}^{-1}$ in ethanol. The activation volume of the complex formation in acetonitrile is 9.4 ± 0.1 $\text{cm}^3 \text{mol}^{-1}$. All the positive values of the activation volume strongly indicate that the ligand substitution reactions on nickel(II) ion proceed via a dissociative-interchange mechanism in these solvents.

Introduction

Activation volumes for solvent exchange on metal ions including transition metals and typical elements in various solvents have been extensively measured by a high-pressure NMR method,^{1,2} while for complex formation there are not as many data of activation volumes.³ Caldin and Greenwood have recently reported volumes of activation for the complexation of nickel(II) ion in nonaqueous solvents by using a high-pressure laser-flash temperature-jump technique.^{3c}

We have studied the mechanism of iron(III) ion complexation on the basis of activation volume obtained by a high-pressure stopped-flow apparatus.^{4,5} The sign of activation

volume for complexation will reflect the character of a metal ion. Thus the high-pressure stopped-flow technique is a powerful and reliable tool for the mechanistic investigation of complex formation. We present a high-pressure study on the complex formation of nickel(II) ion with isoquinoline in various solvents. This paper will provide a unified aspect of the mechanism of nickel(II) ion complexation.

Experimental Section

Solvents. Nonaqueous solvents purchased from Wakojunyaku (Osaka, Japan) were purified just before use. Distilled water was redistilled in the presence of alkaline potassium permanganate. Reagent grade acetonitrile was fractionally distilled twice from a packed column at high reflux ratio over diphosphorus pentoxide (2 g/dm³) and calcium hydride (4 g/dm³). The reflux was performed for 1 h prior to each distillation. Reagent grade methanol was dried over 3A molecular sieves for a few days and then twice distilled.

(1) Merbach, A. E. *Pure Appl. Chem.* **1982**, *54*, 1479 and references cited therein.

(2) (a) Yano, Y.; Fairhurst, M. T.; Swaddle, T. W. *Inorg. Chem.* **1980**, *19*, 3267. (b) Sisley, M. J.; Yano, Y.; Swaddle, T. W. *Ibid.* **1982**, *21*, 1141.

(3) (a) Caldin, E. F.; Grant, M. W.; Hasinoff, B. B. *J. Chem. Soc., Faraday Trans. 1* **1972**, *68*, 2247. (b) Grant, M. W. *Ibid.* **1973**, *69*, 560. (c) Caldin, E. F.; Greenwood, R. C. *Ibid.* **1981**, *77*, 773.

(4) Ishihara, K.; Funahashi, S.; Tanaka, M. *Inorg. Chem.* **1983**, *22*, 194.

(5) Funahashi, S.; Ishihara, K.; Tanaka, M. *Inorg. Chem.*, **1983**, *22*, 2070.